Guided Lamb Wave Propagation in Composite Plate/Concrete Component

Kritsakorn Luangvilai[1]; Wonsiri Punurai[2]; and Laurence J. Jacobs, M.ASCE[3]

Abstract: This research examines the propagation of guided Lamb waves in fiber-reinforced polymer (FRP) bonded components, establishing the effectiveness of combining laser ultrasonic techniques with a time frequency representation (TFR) to experimentally measure the dispersion curves of a concrete component repaired with a FRP plate. A TFR is used to operate on experimentally measured, guided Lamb waves to resolve a FRP bonded component's individual modes and generate its dispersion curves. The objective of this research is to demonstrate that it is possible to develop the dispersion curves of FRP bonded components from a single, experimentally measured guided Lamb wave. The experimental results show that the stiffer the bond, the more deviation from the behavior of a free plate specimen, and the less modes that are present.

DOI: 10.1061/(ASCE)0733-9399(2002)128:12(1337)

CE Database keywords: Wave propagation; Composite materials; Polymer concrete; Plates.

Introduction

A rehabilitation method that has gained widespread acceptance over the last decade involves externally bonding fiber-reinforced polymer (FRP) plates onto the tension face of a concrete beam or slab, thus increasing the beam's (or slab's) flexural stiffness and load capacity. The increased usage of FRP plates in this application has created the requirement for reliable nondestructive evaluation (NDE) techniques that are capable of characterizing these bonded components. The most critical element from a quality assurance (and thus NDE inspection) point of view is the adhesive bond layer—as opposed to the FRP plate itself. Concrete repair procedures typically use a high-quality FRP plate that is manufactured in a controlled environment, while the adhesive bond layer is field assembled and installed, often under adverse conditions. Ultrasonic inspection has great potential in this application, but conventional ultrasonic methodologies (such as pulse echo) are ineffective in interrogating *large* bonded areas. An alternative uses guided Lamb (plate) waves—the primary advantage with guided ultrasonic waves is that they propagate long distances, enabling the efficient interrogation of large bonded areas, including inaccessible regions.

[1]Graduate Research Assistant, School of Civil and Environmental Engineering, Georgia Institute of Technology, Atlanta, GA 30332-0355.

[2]Graduate Research Assistant, School of Civil and Environmental Engineering, Georgia Institute of Technology, Atlanta, GA 30332-0355.

[3]Professor, School of Civil and Environmental Engineering, Georgia Institute of Technology, Atlanta, GA 30332-0355 (corresponding author). E-mail: laurence.jacobs@ce.gatech.edu

Note. Associate Editor: Franz-Josef Ulm. Discussion open until May 1, 2003. Separate discussions must be submitted for individual papers. To extend the closing date by one month, a written request must be filed with the ASCE Managing Editor. The manuscript for this technical note was submitted for review and possible publication on January 23, 2002; approved on April 2, 2002. This technical note is part of the ***Journal of Engineering Mechanics***, Vol. 128, No. 12, December 1, 2002. ©ASCE, ISSN 0733-9399/2002/12-1337–1341/$8.00+$.50 per page.

A waveguide is a component with two (or more) parallel boundaries which ''guide'' ultrasonic waves in the direction of the waveguide (layer). The resulting guided wave exhibits geometric dispersion—different frequencies propagate with different group velocities, causing a change in shape as a wave ''pulse'' propagates. As a result, guided waves consist of many different modes that each propagate independently through a layer. Guided waves are best examined in terms of dispersion curves, which present the relationship between frequency and group velocity (or wave number) for each of the infinite number of modes possible in a particular waveguide. These dispersion curves are governed by a combination of the plate's material properties (elastic moduli and density) and thickness. A multilayered system made up of a number of platelike elements—such as these FRP bonded components—will also act as a waveguide, and its corresponding dispersion relationship depends on the material properties and thickness of each layer, as well as the boundary conditions (quality of the bond) between each layer. The dispersion relationships for layered systems such as these bonded FRP components can be analytically formulated and solved numerically, see Pavlakovic et al. (1997); Rose (1999); or Seifried et al. (2002) for details.

Since the theoretical dispersion curves of a FRP bonded component are directly related to its adhesive bond layer properties (such as bond stiffness, thickness, and adhesion), the accurate measurement of a FRP bonded component's dispersion curves can provide critical, quantitative information about bond quality. Note that these dispersion curves are also dependent upon the properties of the FRP plate layer, but this plate information is not as critical from an NDE perspective. It is impossible to directly measure dispersion curves, but instead, what is typically measured is a time-domain signal (guided Lamb wave) that consists of the superposition of all the modes that travel through the waveguide. This time domain signal is then operated on with signal processing methodologies such as a time frequency representation (TFR) to generate the dispersion curves.

This research examines the propagation of guided Lamb waves in FRP bonded components, establishing the effectiveness

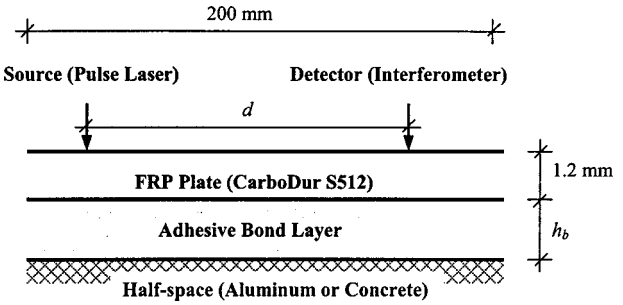

Fig. 1. Schematic of fiber-reinforced polymer bonded component, plus laser source and detection interferometer

of combining laser ultrasonic techniques with a TFR to experimentally measure the dispersion curves of a FRP bonded component. The high-fidelity, broad-bandwidth, and noncontact nature of laser ultrasonics are critical for the success of this study, making it possible to experimentally measure transient Lamb waves in FRP bonded components without any frequency biases. A TFR is then used to operate on this time domain Lamb wave to resolve the FRP bonded component's individual modes and generate its dispersion curves. The objective of this research is to demonstrate that it is possible to develop the dispersion curves of FRP bonded components from a single, experimentally measured guided Lamb wave.

Previous research has shown that a TFR based on the short-time Fourier transform (STFT), the reassigned spectrogram, is particularly well suited for representing Lamb waves, Neithammer et al. (2001). This particular TFR is effective in this application because of its constant time frequency resolution over all times and frequencies. Neithammer et al. (2001) show that the reassigned spectrogram can be used to develop the dispersion curves of a multimode Lamb wave from a single time domain signal. There has been extensive research into the characterization of adhesive bonds (e.g., Heller et al. 2000), but there is less information on guided waves in FRP bonded components. Recently, Kundu et al. (1999) used longitudinal waves and Lamb waves to image defects in FRP plates bonded to concrete. Lowe and Cawley (1994) analyzed the sensitivity of adhesive bond properties on guided waves, showing that the resulting dispersion curves are relatively insensitive to the properties of the adhesive bond layer when the adherend layer is much stiffer.

Experimental Procedure and Calculation of Reassigned Spectrogram

This research examines four different specimens identified as free plate, thin-tape, thick-tape, and epoxy specimen. The free plate specimen is simply a single, stress-free FRP plate that is not bonded to anything. This FRP plate is a 1.2-mm thick, unidirectional, carbon fiber composite (CarboDur S512, manufactured by Sika), 50 min×200 mm. The thin-tape specimen consists of this same FRP plate that is bonded to an aluminum half space with a 0.25-mm thick adhesive tape—$h_b=0.25$ mm in Fig. 1. This adhesive tape (F-9473PC adhesive transfer tape manufactured by 3M) enables bonding with a uniformly thick bond layer. The thick-tape specimen only differs from the thin-tape specimen in that its adhesive bond layer consists of five pieces (layers) of the same adhesive tape, for a bond layer thickness (h_b) of 1.25 mm. The epoxy specimen is composed of the same FRP plate that is bonded to a concrete half space with a 3.175-mm-thick epoxy bond layer ($h_b=3.175$ mm) as specified by the manufacturer (Sikadur 30 epoxy). Note that the FRP plate is much stiffer than both the adhesive tape and epoxy bond, but the epoxy bond is much stiffer than the adhesive tape—modulus E (longitudinal) of 165 GPa for the FRP plate versus 5 MPa for the adhesive tape and 4 GPa for the epoxy.

Broad-bandwidth guided Lamb waves are generated in each specimen with a Nd:YAG laser (4–6 ns pulse) and measured with a high-fidelity laser interferometer over a wide frequency range (100 kHz–10 MHz). See Scruby and Drain (1990) for a discussion of laser ultrasonics, and Bruttomesso et al. (1993) for details on the laser interferometer used in this study. The laser source and interferometric detector are located on the same side of the FRP plate, as shown in Fig. 1. The experimentally measured guided waves are discretized with a sampling frequency of 100 MHz, and represent an average of 30 Nd:YAG shots to increase the signal-to-noise ratio (SNR).

These time domain signals are transformed into the time frequency domain using the STFT, essentially chopping the signal into a series of small overlapping pieces. Each of these pieces is windowed (a 384-point long Hanning window) and then individually Fourier transformed. The STFT presents the time frequency relationship of a signal, showing how its frequency content changes with time. The energy density spectrum of a STFT is called a spectrogram, Cohen (1997). The time frequency resolution of each spectrogram is improved with the reassignment method, that concentrates its energy at a center of gravity, Neithammer et al. (2001). The time (t) axis is converted to group velocity (C_g) with the relationship $C_g=d/t$, where d is the propagation distance. This transformation enables a time invariant comparison that is independent of propagation distance.

Experimental Results and Discussion

Fig. 2 shows typical time domain signals measured in each of the four specimens with the same propagation distance, $d=29.9$ mm. The electromagnetic discharge of the Nd:YAG's firing causes a spurious noise spike at $t=0$ which is windowed out of the reassigned spectrogram. All four signals are measured in the longitudinal direction of the FRP plate, so that their propagation is parallel to the fiber direction. In addition, the signals are measured on the centerline of the 50-mm width to minimize reflections from the side edges. An analysis of these four signals shows nearly identical arrival times for the beginning of the signal (the first nonzero disturbance at ≈4 μs, and note that this portion is on the same order as the noise in the epoxy specimen) and the arrival of the Rayleigh wave portion at ≈14 μs. Second, all four signals have similar shapes (the tape and epoxy specimens are more similar to each other than to the free plate), while the amplitude levels in the free plate specimen are about twice as great as those in the other three specimens. The reason for this difference in amplitude levels is that energy leaks into the bond layer and the half space in the (two) tape and epoxy specimens. There appears to be more leakage in the thin-tape and epoxy specimens, than in the thick-tape specimen, since their amplitudes are lower.

The reassigned spectrogram is used to determine the dispersion curves for each specimen to enable a more quantitative comparison and interpretation. Fig. 3 shows the reassigned spectrogram of the time domain signal measured in the free plate specimen, plotted as group velocity (C_g) versus frequency (f). This spectrogram is a contour plot of the square root of the energy

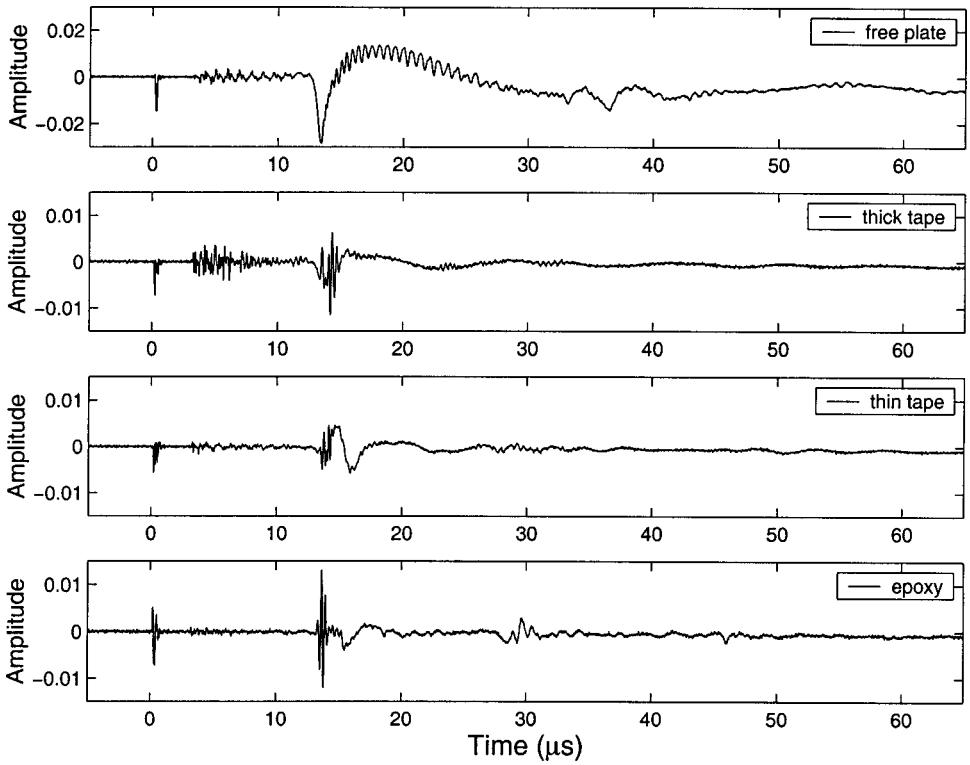

Fig. 2. Time domain signals of free plate, thick-tape, thin-tape, and epoxy specimens (top-to-bottom) for propagation distance of $d=29.9$ mm

density of the STFT, with its peaks corresponding to the dispersion curves of each of the modes that are excited by the laser source. In addition, the free plate's theoretical dispersion curves are plotted as dashed lines in Fig. 3. These theoretical dispersion curves are calculated using the numerical code *Disperse* developed by Pavlakovic et al. (1997), using material properties that are measured independently with bulk ultrasonic waves. This theoretical model treats the FRP plate as a transversely isotropic material, with the propagation direction parallel to the plate's axis of symmetry. There is good agreement between the experimental and theoretical dispersion curves, but these theoretical plots are only included for interpretation of the experimental results.

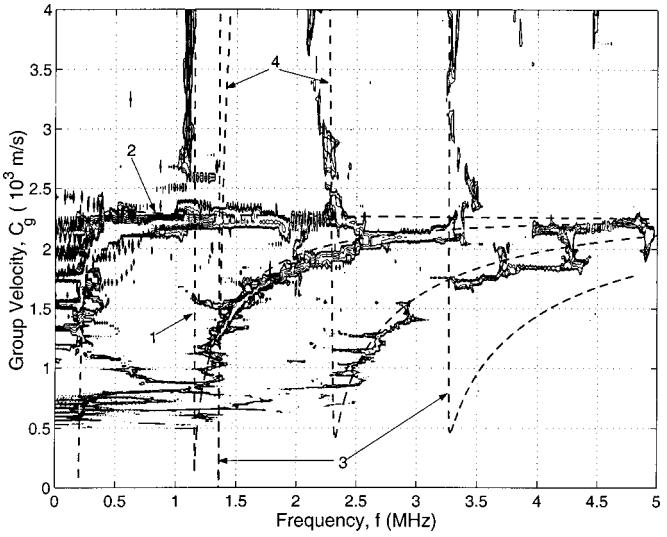

Fig. 3. Contour plot of reassigned spectrogram of time domain signal in Fig. 2 (experimental dispersion curves) for free plate specimen, plus theoretical dispersion curves of free plate specimen (dashed lines)

Overall, the experimental procedure provides excellent definition of the dispersion curves of four modes (identified as 1–4 in Fig. 3) of the free plate specimen. The portions of the spectrogram below a C_g of ≈1,000 m/s that do not correspond to the theoretical modes are due to reflections from the edges of the FRP plate and should be ignored. Next, the low-frequency portions of the spectrogram (below 200 kHz) should also be discounted, because of the lower-frequency limits of the interferometer and near-field effects at these long wavelengths. Note that Modes 1 and 2 converge to the Rayleigh wave velocity ($C_R=2{,}200$ m/s) at high frequencies. The dispersion curves of the stress free FRP plate shown in Fig. 3 can be thought of as the experimentally observable upper limit of a complete disbond; if the FRP plate is disbonded from the half space in the tape or epoxy specimens, the resulting dispersion curves should not possess any more detail than present in the stress free FRP plate of Fig. 3.

Consider the reassigned spectrograms of the thick- and thin-tape specimens, shown in Figs. 4 and 5, with the theoretical dispersion curves of the free FRP plate plotted as dashed lines. First, notice that these two spectrograms are similar to the free plate specimen of Fig. 3; no new modes appear, but there is less definition of the modes that are present. For example, regions of Mode 1 between 1 and 2.5 MHz that are present in Fig. 3, are missing in Figs. 4 and 5. In addition, the dispersion curves of the tape specimens are less distinct—there is a greater C_g-f spread in the modes present in the tape specimens, when compared to the free plate specimen. The overall behavior of the dispersion curves of the two tape specimens is dominated by the attributes of the FRP plate—since the FRP plate is so much stiffer than the adhesive tape (165 GPa versus 5 MPa), the FRP plate acts independently of the aluminum half space in the tape specimens, as far as

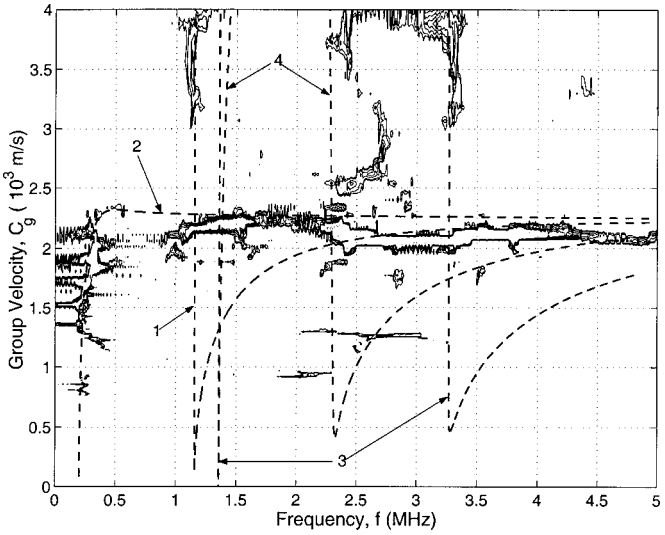

Fig. 4. Contour plot of reassigned spectrogram of time domain signal in Fig. 2 (experimental dispersion curves) for thick-tape specimen, plus theoretical dispersion curves of free plate specimen (dashed lines)

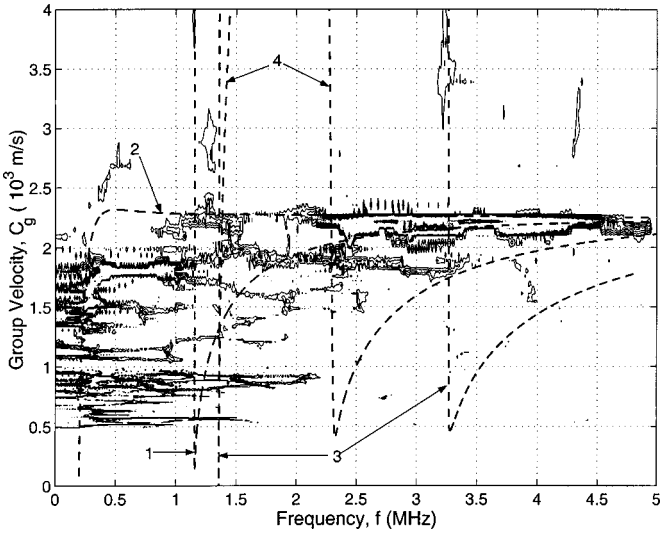

Fig. 6. Contour plot of reassigned spectrogram of time domain signal in Fig. 2 (experimental dispersion curves) for epoxy specimen, plus theoretical dispersion curves of free plate specimen (dashed lines)

these guided Lamb waves are concerned. Fig. 6 shows the reassigned spectrogram of the epoxy specimen, plus the theoretical dispersion curves of the free FRP plate plotted as dashed lines. This spectrogram is significantly different from the spectrograms (dispersion curves) of the other three specimens, consisting of a single mode (Mode 2) through a reduced frequency bandwidth (2–5 MHz). This mode is dominated by the Rayleigh wave contribution, and is practically nondispersive (its C_g is nearly a constant 2,200 m/s). Since the epoxy is so much stiffer than the adhesive tape, this epoxy specimen is more integral from a guided Lamb wave perspective, and thus the FRP plate is more coupled to the concrete half space. Note that the low-signal amplitude of the epoxy specimen (also evident in Fig. 2) causes its spectrogram to be noisier than those of the free plate and tape specimens. The dispersion curves of the thick-tape specimen are more similar to the free plate specimen, than the thin-tape or epoxy specimens, since its adhesive bond layer is the most flexible. This trend is also related to energy leakage—the leakage seems to be most significant in the thin and epoxy specimens. Note that this pattern of leakage is also evident in the time domain signals of Fig. 2, but it is easier to track these trends with the dispersion curves (spectrograms).

This behavior is important from an NDE perspective; if the bond between the FRP plate and the concrete is good, the spectrogram will approach that of the epoxy specimen in Fig. 6, primarily consisting of a single mode, with a C_g that approaches C_R. If, on the other hand, there is a disbond (or if the bond is of poor quality), the resulting spectrogram will approach that of the free plate specimen in Fig. 3, and the dispersion curves will have more modes. In general, the stiffer the bond, the more deviation from the behavior of the free plate specimen and the less modes that are present. Finally, consider the vertical portion of Mode 1, at a frequency of 1.1 MHz. There is a frequency shift to the left (to a lower frequency) in this mode when comparing the thin-tape specimen to both the free plate and thick-tape specimens. This frequency shift to the left for stiffer bonds might provide a more quantitative means to track bond stiffness.

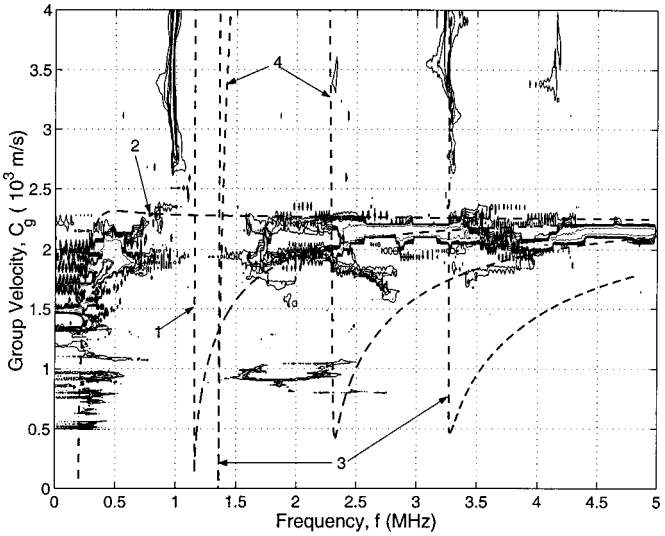

Fig. 5. Contour plot of reassigned spectrogram of time domain signal in Fig. 2 (experimental dispersion curve) for thin-tape specimen, plus theoretical dispersion curves of free plate specimen (dashed lines)

Conclusion

This research demonstrates that the combination of laser ultrasonics with the reassigned spectrogram is very effective in experimentally measuring the dispersion curves of FRP bonded components. The high-fidelity and broad-bandwidth nature of laser ultrasonics makes it possible to experimentally measure transient Lamb waves in FRP bonded components without any frequency biases. The reassigned spectrogram enables the quantitative interpretation of these Lamb waves, making it possible to obtain the dispersion curves of a concrete component repaired with a FRP plate from a single, experimentally measured guided Lamb wave.

The experimental results show that if the bond between the FRP plate and the concrete is good, the measured dispersion relationship primarily consists of a single mode with a C_g that approaches C_R. If, on the other hand, there is a disbond (or if the bond is of poor quality), the measured dispersion relationship will consist of more modes, and will approach that of a free FRP plate specimen. In general, the stiffer the bond, the more deviation from the behavior of the free plate specimen and the less modes that are present. The epoxy and thin-tape specimens are more leaky, have less amplitude and have more divergence from the free plate specimen. Finally, it might be possible to use frequency shifts in a few select modes to monitor (in situ) changes in bond stiffness.

Acknowledgment

This work was partially supported by the National Science Foundation through Grant No. CMS-0201283.

Bruttomesso, D. A., Jacobs, L. J., and Costley, R. D. (1993). ''Development of an interferometer for acoustic emission testing.'' *J. Eng. Mech.*, 119(11), 2303–2316.

Cohen, L. (1995). *Time-frequency analysis*, Prentice-Hall, Englewood Cliffs, N.J.

Heller, K., Jacobs, L. J., and Qu, J. (2000). ''Characterization of adhesive bond properties using Lamb waves.'' *NDT & E Int.*, 33, 555–563.

Kundu, T., Ehsani, M., Maslov, K. I., and Guo, D. (1999). ''C-scan and L-scan generated images of the concrete/GFRP composite interface.'' *NDT & E Int.*, 32(2), 61–69.

Lowe, M. J. S., and Cawley, P. (1994). ''The applicability of plate wave techniques for the inspection of adhesive and diffusion bonded joints.'' *J. Nondestruct. Eval.*, 13(4), 185–200.

Niethammer, M., Jacobs, L. J., Qu, J., and Jarzynski, J. (2001). ''Time-frequency representations of Lamb waves.'' *J. Acoust. Soc. Am.*, 109(5), 1841–1847.

Pavlakovic, B. N., Lowe, M. J. S., Alleyne, D. N., and Cawley, P. (1997). ''Disperse: A general purpose program for creating dispersion curves.'' *Review of progress in quantitative NDE*, D. O. Thompson and D. E. Chimenti, eds., Vol. 16, Plenum, New York, 185–192.

Rose, J. L. (1999). *Ultrasonic waves in solid media*, Cambridge University Press, Cambridge, England.

Scruby, C. B., and Drain, L. E., (1990). *Laser ultrasonics: Techniques and applications*, Adam Hilger, Bristol, England.

Seifried, R., Jacobs, L. J., and Qu, J. (2002). ''Propagation of guided waves in adhesive bonded components.'' *NDT & E Int.*, 35, 317–328.